International Journal of Heat and Mass Transfer 125 (2018) 610–617

Contents lists available at ScienceDirect

International Journal of Heat and Mass Transfer

journal homepage: www.elsevier.com/locate/ijhmt

Heat transfer of aqueous salt solution layers

S.Y. Misyura *

National Research Tomsk Polytechnic University, pr. Lenina 30, Tomsk 634050, Russia
Institute of Thermophysics Siberian Branch, Russian Academy of Sciences, Lavrentiev Ave. 1, Novosibirsk 630090, Russia

ARTICLE INFO

Article history:
Received 6 January 2018
Received in revised form 21 March 2018
Accepted 22 March 2018

Keywords:
Aqueous salt solution
Evaporation rate
Heat transfer

ABSTRACT

Heat transfer and evaporation of layers of water and aqueous solutions of salts on a heated horizontal wall were studied experimentally. Aqueous solutions of salts can be divided into two characteristic groups. For the first group of salts, the evaporation rates and heat transfer coefficients increase with time. For the second group, the rate of evaporation falls sharply with increasing salt concentration and with decreasing liquid layer height. This difference in salts' behavior is determined by the difference in equilibrium curves and in physical and chemical properties of salts. The heat transfer coefficient for water and salt solutions increases when the layer height becomes less than 1.2–1.5 mm. With increasing concentration of salt and when approaching the crystallization point the role of free convection in the liquid phase decreases sharply, and the Nusselt number approaches 1. For salt solutions (LiBr, $CaCl_2$ and LiCl), a significant excess of convection (α) over the conductive heat transfer (λ) is observed for the layer height δ over 1.8–2.0 mm. For pure water, convective and conductive components are comparable even for δ = 3 mm. This difference for salts is associated with substantial intensification of heat transfer, which is probably caused by the concentration flow of Marangoni Ma_C. Strong influence of Ma_C on heat and mass transfer in a thin layer and at high temperatures is detected for the first time and is extremely important for accurate modeling in unsteady and non-isothermal processes. Experimental data show a surprising result. The free liquid convection for salt solutions significantly exceeds the convection in the water layer for the most part of the evaporation time.

1. Introduction

Evaporation of aqueous salt solutions is widely observed in nature, biology and medicine. Evaporation of highly concentrated salt solutions is accompanied by appearance of a new crystalline phase in the form of crystalline hydrates and salt crystals [1,2]. High-temperature evaporation of LiBr salt solutions results in formation of salt crystalline hydrates and may lead to crystalline plugs. Evaporation and absorption of water in aqueous salt solutions of LiBr; $CaCl_2$; LiCl are used in desorbers and absorbers of heat pumps [3].

The evaporation rate of solutions depends on many factors: the temperature of the free surface of the liquid, the concentration of the components, the thermophysical properties of the wall heater [4], wettability [5], the pressure of the external medium [6], as well as on the convection in the gas and liquid phase [7]. Thermophysical features of convection in gas and evaporation were presented in [8]. At evaporation of a thin layer on a heated wall, the important role is played by gas convection and external turbulence, which accelerates drying and intensifies heat and mass transfer [9]. A structural wall influences evaporation and convection in a liquid layer [5]. Stability and break-up of a thin liquid film on structured surface is discussed in [10]. The effect of wettability on evaporation and crystallization was considered in [11–13].

The behavior of aqueous salt solutions significantly differs from the behavior of multicomponent volatiles liquids [14,15]. At evaporation of aqueous salt solutions only water evaporates, and salts remain in the solution. The rate of evaporation of water solutions of salts decreases with time due to the increase in salt concentration. In most studies the numerical simulation of heat and mass transfer processes in a thin film of aqueous salt solutions does not take into account convection in the gas and liquid phases [16–18]. Modeling of heat transfer conditions in lubricant emulsions was considered in [19]. The dependence of the physical properties of solutions on concentration of salts is discussed in [20–23]. Experimental assessment of a hydrophobic membrane-based desorber/condenser with LiBr aqueous salt solution for absorption systems was presented in [24]. The efficiency of transfer processes in the adsorbers of heat pumps depends on the Marangoni flow. The addition of low concentrations of the surfactant leads to a sharp increase in convection in a thin layer of aqueous solution of LiBr

* Address: National Research Tomsk Polytechnic University, pr. Lenina 30, Tomsk 634050, Russia.
E-mail address: misura@itp.nsc.ru

https://doi.org/10.1016/j.ijheatmasstransfer.2018.03.075
0017-9310/

[25,26].The Marangoni flow leads to a film rupture in the absorber and to a decrease in the efficiency of heat transfer [27].

Thus, most studies of absorption and evaporation related to the salt LiBr and, partly, to salts $CaCl_2$ and LiCl, used in absorption heat pumps. Previously, we studied high-temperature evaporation of drops of these salts. In the literature, there is very little data on non-isothermal evaporation of fixed layers when the layer height and salt concentration change several times. Of course, the description of droplets and films is significantly different. In drops, the temperature gradient on the interface and the characteristic size of the convective motion are more clearly determined. In the layers, in addition to the layer height, there is a longitudinal size of the circulation motion, which can significantly differ from the layer length (the heater radius). Thus, experimental data are needed to determine the characteristic convective dimensions and Marangoni numbers for fixed layers. In addition, there is no comprehensive systematic study of a wide range of salts in the literature, when heat transfer and evaporation of aqueous solutions of salts with a strong change in physical and chemical properties are studied in one experiment. Studies of this article help to determine the key parameters that affect the behavior of different salt solutions.

Based on the above the following conclusions may be drawn. The lack of local data on heat and mass transfer of thin layers and films of the salt solutions significantly complicates the development of adequate physical models. Typically, the profiles of concentration, velocity and temperature do not take into account the change of the film thickness and concentration over time. The present work analyzes the impact of various key factors on the heat and mass transfer in a thin layer, when the salt concentration and the layer height change many times.

2. Measuring technique

For the experiments we used aqueous salts solutions: LiBr, $CaCl_2$, LiCl, NaCl, CsCl, $BaCl_2$, and $MgCl_2$. The initial height of the solutions was 3 ∓ 0.1 mm. The experiments were carried out at ambient air temperature of 24 °C; relative air humidity of 40%; and ambient air pressure of 1 bar. The working section (1) was titanium alloy with diameter $d = 70$ mm (Fig. 1).

The aqueous salt solutions (3) were placed on a horizontal heated wall of the working section. The experimental setup was located in a box with dimensions: 1 m × 1 m × 1 m. The upper part of the box was open to prevent changes in air humidity. The sidewalls of the box prevented the effect of convection of external air in the room and made the measurements more time-stable. The measurement of external humidity and ambient temperature showed no change in time.

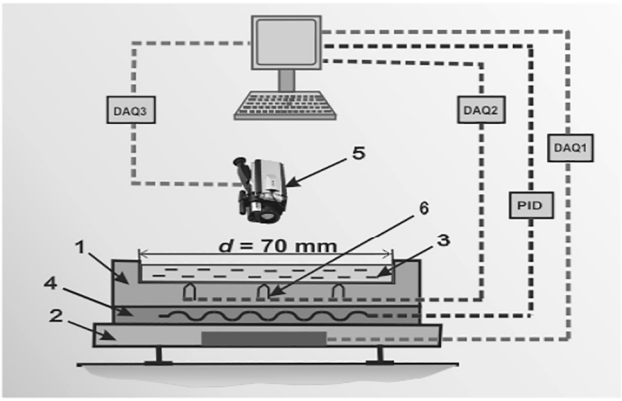

Fig. 1. The experimental setup: 1 – titanium working section; 2 – electronic balance; 3 – liquid; 4 – heater; 5 – thermal imager; 6 – thermocouple.

Thermocouples (6) for wall temperature measurement were located near the wall surface (0.5 mm from the wall surface). The wall temperature T_w was kept constant in an automatical regime with accuracy within ±0.5 °C using PID and DAQ. The proportional-integral-derivative controller (PID) allows regulation of the heater power aimed at the achievement of the quasi-permanent wall temperature T_w. The values of the wall temperature are sent by thermocouples (6) to the data acquisition system (DAQ2) and then to the PC and PID. The wall temperature was kept constant automatically with the accuracy of ±0.5 °C. DAQ1 is designed to receive and process data on the droplet mass (a change in the droplet mass is recorded by the scales and the analog signal from the scales (2) is sent to the DAQ1 and PC.) The DAQ3-PC-thermal imager (5) is designed for measuring the temperature of the droplet surface T_s and processing data in the PC using special software that allows determination of the average temperature of a droplet surface. The interfacial temperature of liquid was determined with the help of thermal imager NEC R500 (5) (resolution of infrared camera was 640 × 512 pixels). The spectral bandwidth of infrared camera in short wave range (SW) was 3–5 μm. Before the experiments tests were carried out to evaluate the influence of salt concentration on the thermal imager measuring. The error of thermal imaging measurements associated with a change in salt concentration from 10% to 60–65% was 1–2%. Thus, a change in salt concentration did not affect the temperature measurements. The value of initial mass concentrations of salt in aqueous salt solutions (C_{01}) was determined using the densimeters. Current salt concentrations C_{1i} of the aqueous salt solutions were determined by a weight method. The setup was placed on the accurate balance (2). Since the salt mass does not change with time, it was easy to determine the current concentration values. As the salt concentration grows with time, the water concentration, on the contrary, decreases over time (C_2–$C_{H_2O} = 1 - C_1$; where $C_{H_2O} = m_{H_2O}/m$; $C_1 = C_{sol} = m_{sol}/m$; m_{H_2O}, m_{sol}, m ($m = m_{H_2O} + m_{sol}$) are the mass of water, salt and aqueous salt solution). The increase in salt concentration leads to the change of the equilibrium partial vapor pressure p_s at the interfacial surface as well. At the known equilibrium values of temperature T_s and equilibrium vapor concentration C_s, the equilibrium vapor density ρ_s is uniquely determined by the equilibrium curves. The maximum error of evaporation rate was 11–12% for large times, when there was low evaporation rate. Experimental study of evaporation rates was conducted before the occurrence of crystallization.

3. Evaporation and heat transfer of aqueous salt solutions

The evaporation rate of the solution layer j was determined for narrow time intervals $\Delta t = t_{i+1} - t_i$ ($j_i = dm_i/dt_i \approx \Delta m_i/\Delta t_i$ (kg/s), where m_i is the current mass of liquid. Experimental data on evap-

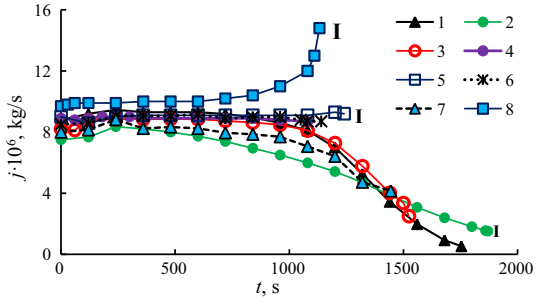

Fig. 2. Evaporation rate of aqueous salt solutions (initial salt concentration $C_{01} = 10\%$; $T_w = 80$ °C): 1 – LiBr; 2 – LiCl; 3 – $CaCl_2$; 4 – NaCl; 5 – CsCl; 6 – $BaCl_2$; 7 – $MgCl_2$; 8 – H_20.

oration rate j are shown in Fig. 2. The graphs show intervals of measurement errors. Curves 1–8 represent evaporation rates for different salt solutions. The following important differences between evaporation curves may be noted. The evaporation rate of salt solutions of $CaCl_2$, LiCl, LiBr and $MgCl_2$ decreases continuously with time (t > 500–800 s). The evaporation rate for water and for salt solutions of CsCl, NaCl, $BaCl_2$ is quasi constant for most part of the evaporation time. Thus, the generally accepted notion that with increasing salt concentration, the evaporation rate falls, is not always true. The salt solutions can be divided into two groups. The first group includes salts $CaCl_2$, LiCl, LiBr and $MgCl_2$, where the evaporation heat increases markedly with increasing concentration. It is important to emphasize that the evaporation of aqueous salt solutions is accompanied by two processes – evaporation and dilution. The evaporation heat substantially exceed the heat of dilution. For the second salts group (CsCl, NaCl, and $BaCl_2$) the evaporation heat weakly depends on concentration. If interaction between molecules of water and salt is significantly higher than the forces between only water molecules, more energy is required to break intermolecular bonds (water and salt) for the phase transition from liquid to vapor. As a result j decreases (salts $CaCl_2$, LiCl, LiBr and $MgCl_2$).

Another important condition of evaporation rate quasi-constancy for the second group is high diffusion rate in the solution. Since the diffusion coefficient D_s in the solution is much less than the diffusion coefficient in the gaseous mixture D_g, the gradient of salt concentration will be high. Obviously, the higher the salt gradient and the lower the D_s, the smaller the rate j. The inertial influence of diffusion for the first group may also cause a significant drop of j. The lowest rate of evaporation (before crystallization) for all investigated salts is achieved for the salt LiBr. This salt is most often used in absorption heat pumps. The lowest evaporation rate uniquely corresponds to the highest absorption activity in the absorber of the heat pump. High absorption rates lead to a noticeable increase in the solution temperature due to phase transition and to a high efficiency of the heat pump. There is a frequent stereotype: the higher the salt solubility, the higher absorption activity of the salt solution, and the solubility clearly controls the kinetics of evaporation (absorption). However, these statements are incorrect. Solubility of salts LiBr and CsCl is high, that allows achieving salt concentrations above 60%. The salt LiBr is applicable in heat pumps for the reasons mentioned above. The salt CsCl evaporates very quickly at high concentrations of salt, and therefore will have a very low absorption rate and a very low degree of solution heating in the absorber. Therefore, this salt (CsCl) is not applicable in heat pumps. All salts of the second group cannot be used in heat pumps. The equation of heat balance for the free liquid surface has the form (1). The heat flux $\alpha_l(T_w - T_s)$ is supplied to the liquid from the heated wall (q_w) (1), and the supplied heat is consumed for liquid evaporation $q_e = rj_e$ ($j_e = \Delta m/F\Delta t$), cooling from gas convection $q_c = \alpha_l (T_s - T_0)$ and radiation q_r,

$$q_w = \lambda_w(dT/dy)_{y=0} = \alpha_l(T_w - T_s) = q_\Sigma, \text{ where}$$
$$q_\Sigma = rj_e + \alpha_g(T_s - T_0) + q_r \quad (1)$$

where m is liquid mass, λ_w is the thermal conductivity of titanium alloy, y is the transverse coordinate to the metal wall (y = 0 corresponds to the surface of the wall, F is the area of the liquid free surface, t is the time, r is the latent heat of evaporation (latent heat of evaporation for aqueous salt solution consists of two heats: the heat of water evaporation and the heat of dilution due to changes in the concentration of salt), α_g is the heat transfer coefficient for vapor-gas mixture, resulting from free gas convection over the surface of the heated liquid, and T_0 is the gas temperature away from the wall. The heat transfer coefficient α_l for the salt solution was determined by the expression (2),

$$\alpha_l = \lambda_w(\Delta T_i/\Delta y)_{y=0}/((T_{wi} - T_{si})) \approx q_\Sigma/(T_{wi} - T_{si}) \quad (2)$$

where ΔT_i is the temperature difference near the surface of the wall of the heated work area, T_{wi} is the current average wall temperature, and T_{si} is the current average temperature of the interfacial surface (liquid–gas). The radiation flux was determined by the expression $q_r = \varepsilon\sigma(T_s^4 - T_0^4)$, where ε is the coefficient of thermal radiation for the fluid; σ is the Stefan-Boltzmann constant. The heat transfer coefficient for gas α_g was determined in accordance with [28] by the expression $Nu = 0.54Ra^{0.25}$ (where Nu and Ra are Nusselt and Rayleigh numbers, $Nu = \alpha_g R/\lambda_g$, $Ra = g\beta\Delta T_s(R)^3/va$, ΔT_s is the temperature gradient on the free surface of the liquid, v is the kinematic viscosity of the liquid, β is the coefficient of thermal expansion, g is the gravity acceleration, α_g is the heat transfer coefficient for gas (air), and R is the characteristic scale (the radius of the cylindrical heater), and λ_g is the thermal conductivity of gas. For water and all salt solutions, the condition of heat balance was performed in accordance with (1) for the most evaporation time. The difference $\Delta_1 = (q_w - q_\Sigma)100\%/q_w$ did not exceed 3–5%. In addition, at small and medium times the impact of gas convection and heat radiation is negligible compared to the heat of vaporization. Therefore, the error in determining the gas convective component (α_g) has almost no effect on thermal balance performance and accuracy of determining α_l. At large times, when the heat transfer coefficient significantly changes over time, the maximum value of Δ_1 reaches 10–15%. The growth of Δ_1 is due to the increase of non-stationarity at large times. The upper surface temperature was measured by the thermal imager. The wall temperature was measured by thermocouples. The maximal measurement error α_l was within 11–13%.

Experimental data on the changes of heat transfer coefficient α_l for water and aqueous salt solutions layers are shown in Fig. 3. The behavior of the coefficient α_l can be also divided into two characteristic groups: (1) for solutions of salts $CaCl_2$, LiCl, LiBr there is an extremum for coefficient α_l. A similar behavior is also specific for the salt $MgCl_2$. The curves for heat transfer have 3 distinctive time stages: the stage with a slightly variable α_l; growing α_l and reaching the extremum; and a continuous decrease in α_l; (2) For water and for the second group of salts CsCl, NaCl the extremum is absent, and there are two stages of evaporation: a quasi-constant heat transfer and continuous increase in α_l. A similar behavior is also observed for the salt $BaCl_2$.

The most intensive heat transfer corresponds to water. For solutions of salts, the coefficient α_l is lower than that of water even at the initial time of evaporation (with low initial salt concentration of 10%). The important fundamental feature of evaporation of solutions of salts of the first group is the existence of extremum for the curve α_l. Since at large times there is a significant change in α_l, a

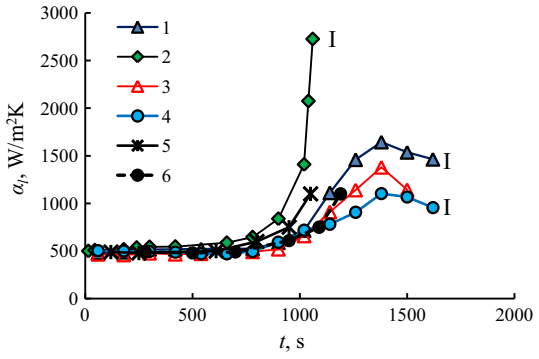

Fig. 3. The heat transfer coefficient α_l for the layer of different aqueous salt solutions (initial concentration of salt C_{01} = 10%; T_w = 80 °C): 1 – LiBr; 2 – H_20; 3 – $CaCl_2$; 4 – LiCl; 5 – NaCl; 6 – CsCl.

non-linear temperature profile occurs in the solid wall, increasing the measurement error. Therefore, to determine the heat flux we used the flux $q_{\sum}$ (at large times). The heat transfer coefficient may be considered as a product of two functions $\alpha_l = cf_1(t)f_2(t)$, $f_1(t) = q_{\sum}$, $f_2(t) = 1/\Delta T_w$ ($\Delta T_w = T_w - T_s$).

Changes in the heat flux $q_{\sum}$ (curves 1, 2) and $1/\Delta T_w$ (curves 3, 4) for LiBr and $CaCl_2$ over time are presented in Fig. 4. Graphs of heat flux $q_{\sum}$ and curves $1/\Delta T_w$ for the two aforementioned solutions of salts have long time periods of quasi-constant values (t = 0–1000 s).

For time t > 1000 s, $q_{\sum}$ continuously decreases, and $1/\Delta T_w$ increases. Such character of the curves leads to the existence of extremum in heat transfer. When approaching the point of crystallization the solution viscosity dramatically increases, which leads to the suppression of thermo-gravitational and thermo-capillary convection. The drop in $q_{\sum}$ is associated with an increase in the concentration of salt and with the approach of the solution to equilibrium (the salt concentration C_s on the free surface of the liquid approaches the equilibrium salt concentration C_s). A similar behavior is specific for the salt $MgCl_2$. The behavior of water and salts NaCl, CsCl and LiCl (Fig. 5) is different from Fig. 4. Thus, Fig. 5 shows the behavior of water, which qualitatively reflects the character of the dependence for aqueous solutions of salts NaCl and CsCl. The curve of the heat flux for water also has a long flat area. However, with a substantial reduction in the layer height (t > 700 s), $q_{\sum}$ for water increases dramatically compared to its decrease for the salts on Fig. 4 and for the salt of LiCl ((1), Fig. 5). And the heat flux for an aqueous solution of LiCl salt has no flat area and $q_{\sum}$ decreases continuously with time. The sharp 1/ΔT increase for LiCl salt starts significantly earlier (t > 700 s) compared to Fig. 4 (LiBr, $CaCl_2$). For the greater part of the evaporation time, the radiation flux and the convective flux are much less than the heat of vaporization. Therefore, the dominant role in the fall of $q_{\sum}$ is caused by a decrease in the flux density j.

To identify the main factors due to which salts are divided into two specified groups, it is necessary to consider the equilibrium

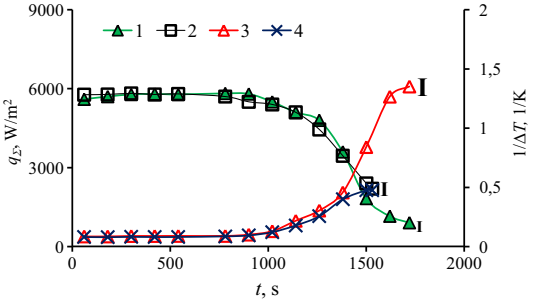

Fig. 4. Changes in heat flux $q_{\sum}$ (1, 2) and $1/\Delta T$ (3, 4) in time (C_{01} = 10%; T_w = 80 °C): 1 – LiBr; 2 – $CaCl_2$; 3 – LiBr; 4 – $CaCl_2$.

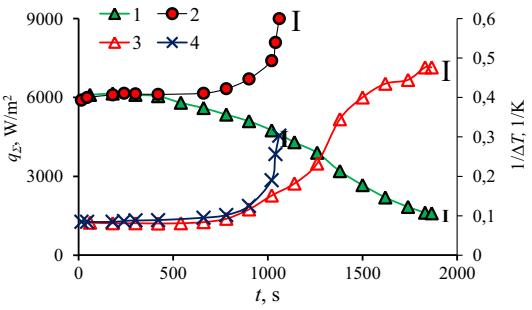

Fig. 5. Changes in heat flux $q_{\sum}$ (1, 2) and $1/\Delta T$ (3, 4) in time (C_{01} = 10%; T_w = 80 °C): 1 – LiCl; 2 – H_2O; 3 – LiCl; 4 – H_2O.

curves and properties of salts, as well as to link these properties with evaporation rate. The evaporation rate of the layer j is associated with the difference in the equilibrium vapor pressure Δp_{vs} ($\Delta p_{vs} = p_{vs} - p_{v,ext}$, where p_{vs} is the vapor pressure at the liquid interface; $p_{v,ext}$ is the vapor pressure in air far from the liquid surface) in accordance with (3) [29]

$$j \sim D_g(\rho_{vs} + \rho_{v,ext})ln(1 + B_M) \sim p_{vs}(if\,\rho_{vs} \gg \rho_{v,ext}) \quad (3)$$

where p_{vs} is expressed through ρ_{vs} using Mendeleev-Clapeyron equation, ρ_{vs} is vapor density of water at the interface surface; D_g is the vapor diffusion coefficient in gas, B_M is the Spalding mass number [29]. In accordance with the equilibrium curves, an increase in the concentration of salt in the salt solution leads to a drop in the equilibrium partial pressure of water vapor p_{vs}. Equilibrium curves vary significantly for different aqueous salt solutions. Table 1 provides data on p_{vs} and the differential enthalpy of dilution.

As can be seen from Table 1, at low salt concentration C_1 = 10–20%, t = 100–200 s) values of p_{vs} for LiBr, $CaCl_2$ and LiCl salts differ slightly. However, with an increase in salt concentration (t = 1200 s), p_{vs} for LiCl salt is significantly lower than for the other two salts. In accordance with (3), the evaporation rate of the aqueous solution of LiCl salt should be noticeably lower, which corresponds to Fig. 2. When approaching the crystallization point, the ratio of the partial vapor pressure changes. The value of p_{vs} for LiCl salt becomes, vice versa, higher than for LiBr and $CaCl_2$ salts. Therefore, the evaporation rate for the aqueous solution of LiCl salt is, on the contrary, higher than that of the other two considered salts (see Fig. 2). This analysis is undoubtedly very approximate and qualitative, since it does not take into account the change in diffusion, viscosity and convection in the liquid, which vary greatly with the increase in salt concentration.

Of interest is the obvious question, how the partial vapor pressure is associated with the properties of salt. To relate the transfer in the liquid and gas phases, it is necessary to consider intermolecular forces near the interface. To turn the liquid into vapor, it is necessary to spend the work ($l = l_1 + l_2$) on breaking intermolecular bonds (l_1) and on gas expansion (l_2). The work $l_1 \gg l_2$ and l_2 is approximately the same for different salts. The work l_1 is determined by van der Waals forces, which determine the interaction between water and salt molecules. On the other hand, the evaporation rate may be associated with energy (heat), which has to be spent on water evaporation. This heat is the sum of the latent heat of vaporization and the heat of dilution. Water evaporation leads to an increase in salt concentration and to additional dilution heat. Both heats lead to liquid cooling at the interfacial surface. To assess the role of evaporation heat, it is necessary to estimate the total number of intermolecular bonds between water and salt molecules. Heat transfer and evaporation are often investigated as a function of the mass concentration of salt. Table 2 shows values of molar masses for the investigated salts.

As can be seen from Table 2, the first group of salts has a substantially lower molecular weight than the second group, with the exception of NaCl salt. Near the liquid interface the number of molecules of CsCl and $BaCl_2$ salts, will be much less (less than the concentration of the molecules) than for the molecules of the

Table 1
The equilibrium vapor pressure of water (p_{vs}) and the differential enthalpy of dilution.

Salt	p_{vs}, bar (t = 100 s)	p_{vs}, bar (t = 500 s)	p_{vs}, bar (t = 1200 s)	H, kJ/kg (t = 1500 s)
LiBr	0.25	0.24	0.17	465
$CaCl_2$	0.25	0.23	0.18	550
LiCl	0.23	0.19	0.08	425

Table 2
Molar mass (M) of salt.

I group					II group		
Salt	LiBr	$CaCl_2$	LiCl	$MaCl_2$	CsCl	$BaCl_2$	NaCl
M, g/mol	87	111	42	95	168	172	58

salt of the first group. Then the number of bonds (short-range and long-range) between water molecules and CsCl and $BaCl_2$ molecules will be much smaller than for the first group. In this case, most of the water molecules will be removed from the liquid surface (turn into vapor) without interaction with the salt molecules, and the total effect of the dilution heat will be lower. Then p_{vs} (at a constant mass concentration of salt) will be significantly higher for the second group than for the first one. Therefore, according to (3), for the second group j will be noticeably higher than for the first group (see Fig. 2).

Molar mass of NaCl salt is low and does not correspond to this analysis, which is easily explained. For aqueous solution of NaCl salt under the conditions of this experiment crystallization begins approximately at salt concentration $C_1 = 26\%$. This salt has a very low solubility. At such low concentration and low dilution heat, this salt solution will have a slightly lower evaporation rate than water. The crystallization point for CsCl and $BaCl_2$ salts will also correspond to the mass concentration of the salt, which is much lower than for the salts of the first group. If we relate the crystallization point not to the mass, but to the volume concentration of salt, the difference in solubility between the second and third groups will be even greater. Thus, the second group of salts for any time t and at any temperature T_s has much less water-salt intermolecular bonds. Then water molecules can move more freely in the transverse direction to the free liquid surface, i.e. the solution can be considered in the first approximation as having an infinite diffusion. Then the diffusion equation may be skipped, limiting only to the momentum transfer and the energy equations. For the first group, the diffusion equation with variable boundary conditions has to be solved (the equilibrium partial vapor pressure at the interfacial boundary and the difference ΔT_w change several times over time).

The evaporation rate is undoubtedly associated with the heat and mass transfer rate, which is regulated by diffusion, viscosity, dilution heat (Table 1) and the intensity of convective motion in the liquid. A higher concentration of salt molecules for group 1 will result in a higher gradient of C_1 near the interface (liquid–gas). Our experimental data show that before crystallization in salts of group 1, the average salt concentration (throughout the solution volume) is 10–15% lower than for the equilibrium crystallization curve. The supersaturation in all experiments did not exceed 0.1%. As a result, there is a high transverse gradient of salt concentration near the free surface of the solution. It is surprising that such a high gradient corresponds to the liquid layer thickness of 0.3–0.5 mm. Thus, a high gradient at a distance of 0.01–0.1 mm from the interface results in a higher diffusion water flow.

It is surprising that even before crystallization, despite the stronger bonds of water and salt molecules, the derivative of the evaporation rate decreases only slightly.

Usually, when modeling in a thin layer of the solution, a linear profile of temperature and concentration is taken. However, this approximation can only agree with the transverse temperature profile (temperature gradient before the beginning of crystallization of $\Delta T_w = T_w - T_s = 1$–$4$ °C). The concentration gradient is highly nonlinear, which is important to take into account when modeling, as this will lead to a change in the transverse mass flow depending on the transverse coordinate. This fact is especially important to consider when modeling crystallization in a thin layer, e.g., at the formation of nano-coatings with a strictly defined morphology. The high transverse concentration gradient will lead to different transverse crystal growth rates and will contribute to the increase of crystal defect and deterioration of the coating properties.

The development of modern technologies dealing with high rates of thin layer evaporation needs experimental data on local profiles of concentrations and velocity in the liquid. To date, these studies are extremely difficult. Theoretical and experimental investigations in this area are the subject of further study.

Qualitative behavior of the evaporation rate (for aqueous salt solutions) over time may be easily analyzed with the simplified expression for the isothermal case and for a thick layer of water (4) [3]

$$j_1 = -\rho D\left(\frac{\partial C_2}{\partial y}\right)_{y=0} = \frac{\rho\sqrt{D}}{\sqrt{\pi t}}(C_{02} - C_{0s}), \tag{4}$$

where ρ is the density of aqueous salt solution, D is the diffusion coefficient in aqueous salt solution, t is the time, C_{02} is the initial water concentration in aqueous salt solution, C_{0s} is the water equilibrium concentration for liquid free surface and for $T = T_0$ (T_0 is the initial temperature of the solution). As can be seen from (4), even if the diffusion coefficient does not change, there will be a continuous decrease in the mass flux density of water over time, and, accordingly, a continuous decrease in the evaporation rate. The driving force of desorption ($\Delta C = C_{02} - C_{0s}$) over time decreases as the thermodynamic system approaches equilibrium.

The ratio of convection (convection in liquids) and conduction (molecular transfer in the absence of the mean motion of the medium) is dependent on the height of the liquid layer δ. With decreasing δ the role of convection decreases. Fig. 6 shows experimental data of δ changes on time for water and salt solutions of LiBr, $CaCl_2$, LiCl. The height of the layer δ was determined experimentally by the expression $\delta = m/\rho F$, where m is the current liquid mass, ρ is the liquid density, and F is the surface area of the liquid). The decrease of the mass m was registered by weights. The evaporation area was constant for all experiments (experiments were carried out before the water film rupture).

For water, the derivative of the layer height on time $d\delta/dt$ is quasi-permanent for entire period of evaporation. For salts solutions, a derivative decreases approaching the point of crystallization that is due to a sharp decrease in the evaporation rate (Fig. 2). The data for the minimum layer height δ_1 are represented on Fig. 7.

Height δ_1 for water corresponds to time when the water film ruptures and forms a dry spot on a solid wall, and δ_1 for salt solutions is taken for time when salt crystallization starts on the free liquid surface. For the case of salts, the rupture was not observed.

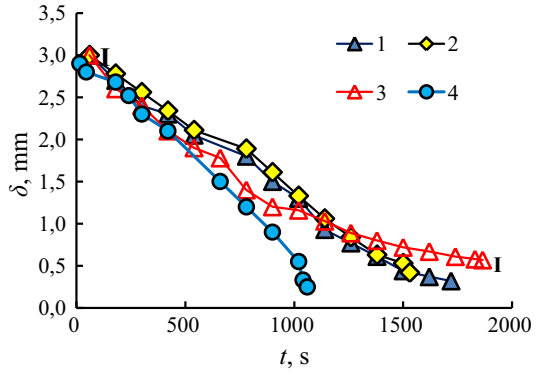

Fig. 6. Change in the liquid layer height versus time ($C_{01} = 10\%$; $T_w = 80$ °C): 1 – LiBr; 2 – $CaCl_2$; 3 – LiCl; 4 – H_2O.

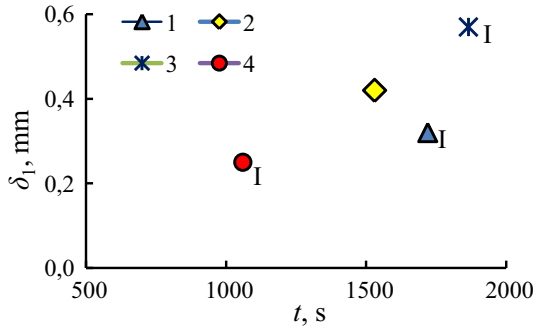

Fig. 7. The minimum height of the liquid layer (C_{01} = 10%; T_w = 80 °C): 1 – LiBr; 2 – $CaCl_2$; 3 – LiCl; 4 – H_2O.

According to the graphs, the minimum value of δ_1 corresponds to the water (4). For salts (1–3), the minimum height corresponds to the aqueous solution of LiBr.

We define the dimensionless criteria for the liquid phase, characterizing the convection intensity in the liquid. The Rayleigh number $Ra = GrPr = g\beta\Delta T_s(L_{TL})^3/\nu a$ ($Pr = \nu/a$, $Gr = g\beta\Delta T_s(L_{TL})^3/\nu^2$, ΔT_s is the temperature gradient on the free surface of the liquid, ν is the kinematic viscosity of the fluid, β is the coefficient of thermal expansion, g is the gravity acceleration, L_{TL} is the characteristic scale (subscripts T and L refer to the temperature and to the liquid). To estimate the values of Rayleigh number and the thermal Marangoni number (Ma_T) for convection in a water layer, a characteristic convective thermal scale was determined. It is assumed that the order of the thermal scale values should coincide with the speed scale (the liquid circulation scale inside the layer).

When measuring with a thermal imager, it is necessary to estimate the influence of the wall on the measurement of the liquid surface temperature and the influence of salt concentration on the measurement error [30–33]. In all experiments, the height of the water layer and the aqueous salt solution exceeded the value when it is necessary to take into account the influence of the wall. The effect of the salt concentration on the measurement of temperature T_s, as mentioned earlier, is within the error of the thermal imager.

Fig. 8(a) presents a thermal image of the water layer surface, and Fig. 8(b) shows a multi-magnified image of the temperature region (A) on the free surface of the liquid. At magnifying one can clearly see the characteristic scales (temperature inhomogeneity) with a size L_{TL} = 3–5 mm. The temperature gradient along these inhomogeneities is 0.3–0.5 °C. The value of L_{TL} is approximately 2 times greater than the height of the water layer. When the Ra value was determined for air (moving over the surface of a hot liquid), the characteristic size (L_{TG}, where the index G refers to gas (air)) was equal to the radius of the cylinder, i.e. 35 mm.

For convection in a thin layer of liquid, it is incorrect to take the value of the specified radius R_0 (the radius of the cylindrical heater). In this case, $Ra = 1.2\cdot10^7$ (L_{TL} = 35 mm, the maximum temperature gradient at a distance from the liquid edge to its center is approximately 3 °C). With such a large Ra value, an intense convection should be observed in the final evaporation stage. However, as further will follow from Fig. 9, for time t > 700–800 s the value of Nu number is close to unity. It is obvious that the circulation flow, when its longitudinal size is much larger than the transverse one, is unstable to disturbances (for time t = 1000 s, R/δ = 35 mm/0.5 mm = 70, where δ is the height of the water layer (Fig. 6)).

We determine the values of Ra and Ma_T for water and for the layer height δ, when δ is close to the maximum value (t = 300 s), as well as for the lowest height δ (t = 1050 s). At the length of the characteristic convective scale L_{TL} = 4 mm, and the temperature gradient ΔT_s = 0.5 °C. In accordance with the above (for time t = 300 s) Ra = 3000, the thermal Marangoni number $Ma_T = (\Delta T_s L_{TL}/\mu a)\cdot(d\sigma/dT_s)$ = 5100, where σ is the surface tension of the liquid, L_{TL} = 4 mm, and ΔT_s = 0.5 °C. For the time t = 1050 s Ra = 0.6 and Ma_T = 100 ($L_{TL} = 2\delta$ = 0.4 mm, ΔT_s = 0.1 °C). Thus, at small evaporation times (δ = 2.2 mm), the Ra and Ma_T numbers exceed the critical value 1000–2000, at which the free-convective motion of the liquid occurs [28]. For the final stage of water evaporation (t = 1050 s), the values of Ra and Ma_T are much lower than the specified critical value 2000, and therefore there is no convection in the water layer. Heat transfer is determined only by conductive heat transfer.

Determining the solutal Marangoni number (Ma_C) is quite difficult, because it is difficult to measure the concentration gradient ΔC_s on the liquid surface in a thin layer. $Ma_C = (\Delta C_s L_{TL}/\mu D)\cdot(d\sigma/dC_s)$, where C is the salt concentration and D is the diffusion coefficient in the aqueous salt solution. However, the Ma_C value may be determined at a very low gradient of salt concentration on the liquid surface. Let ΔC_s = 0.1%, then Ma_C = 100,000 for the initial evaporation period (δ = 3 mm, $L_{TL} = 2\delta$ = 6 mm) and for the salt solution an intense solutal Marangoni flow will be observed on the free surface. Thus, the solutal Marangoni number plays a crucial role in the heat exchange of the salt solution. An intense solutal Marangoni convection is due to the fact that the diffusion coefficient D is almost two orders of magnitude lower than the thermal diffusivity coefficient a. As a result, if there is a gradient ΔT_s, the evaporation rate gradient on the surface of the liquid and, accordingly, the salt

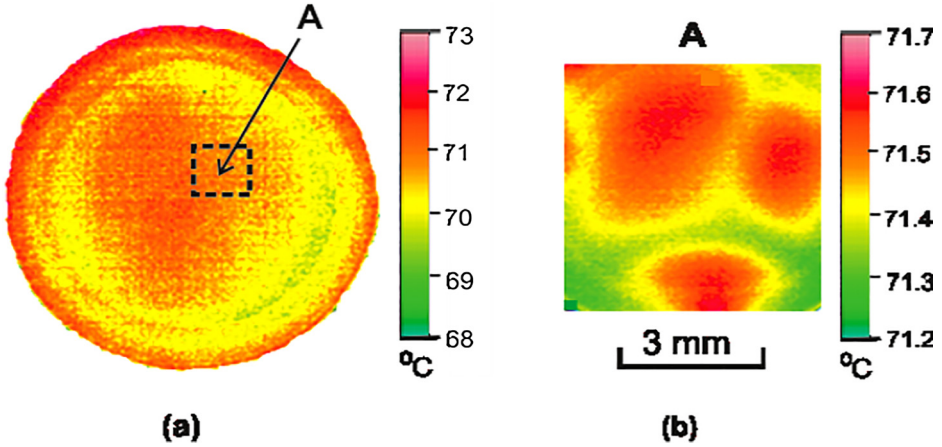

Fig. 8. Thermal imager photos for (T_w = 80 °C, t = 300 s): (a) Area A shows the location on the water layer surface; (b) Thermal image of the area A at multiple magnification.

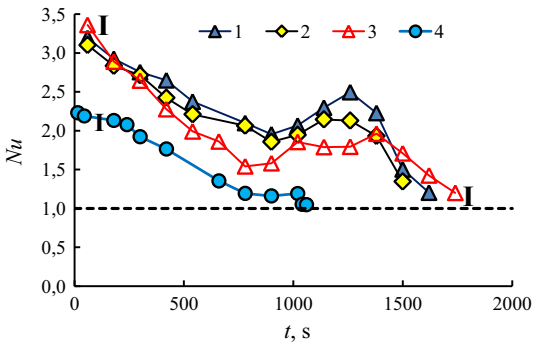

Fig. 9. Changes in the Nusselt number *Nu* over time (C_{01} = 10%; T_w = 80 °C): 1 – LiBr; 2 – $CaCl_2$; 3 – LiCl; 4 – H_2O.

concentration gradient ΔC_s will also appear. The surface area where water evaporates faster will have a higher salt concentration. Thus, curves for salt solutions, taking into account the solutal Marangoni convection inside the layer, should be higher than for water.

Fig. 9 shows changes in the dimensionless values of the heat transfer coefficient α_l in the form of Nusselt number *Nu* ($Nu = \alpha_l\delta_l/\lambda_l$). The increase of heat transfer is directly proportional to the growth of convection only if the boundary conditions do not change, i.e., the height of the liquid δ_l is constant. In the considered cases, its height decreases almost 10 times during evaporation. In this case, the simulation is significantly complicated. At the evaporation beginning, the free convection dominates over the conduction heat transfer. In the final stage of evaporation, when the height of the layer becomes low enough (0.2–0.5 mm), heat transfer due to thermal conductivity is predominant. For solutions it is necessary to estimate the value of the solutal Marangoni number, which can be many times greater than the *Ra* value and the thermal Marangoni number.

Experimental data show a surprising result. In the initial period of evaporation, when the height of the layer of water and all solutions is the same (δ_{0l} = 3 mm), the convection for all salt solutions significantly exceeds the convection in the water layer. It is important to note that the first point on all graphs corresponds to time t = 40–60 s. Therefore, the *Nu* value does not agree with the time close to 1–10 s. It is not correct to approximate the curve for *Nu* with a straight line to get the value of *Nu* for t = 0. Our further paper, which is to be published soon, will show that the highest derivatives of $d\alpha/dt$ and dNu/dt correspond to small times when the solution is heated. In this moment, the highest Marangoni forces arise on the surface of the liquid layer.

The values of *Ra*, Ma_C и Ma_T have been estimated above, and it is shown that Ma_C prevails in the initial evaporation period, which explains the excess of curves 1–3 (aqueous solutions of salts) over curve 4 for water. We decompose the numerator in the expression for *Nu* ($Nu = \alpha_l\delta_l/\lambda_l$) into two components $\alpha_l\delta_l = \alpha_1 + \alpha_2 = \alpha_l\delta_l + \lambda_l$. If $\alpha_l\delta_l \gg \lambda_l$, then the numerator is determined only by convection. If $\alpha_l\delta_l \ll \lambda_l$, then the numerator is determined only by thermal conductivity (Nu = 1). Then, in the initial evaporation period (t = 50–100 s), for water (curve 4 in Fig. 9) components α_1 and α_2 are comparable. The contribution of convection to heat transfer slightly exceeds the contribution from molecular transfer (from conductive transfer, which is characterized by λ_l). For aqueous solutions of salts (t = 50–100 s, curves 1–3 in Fig. 9), the effect of free convection (due to Ma_C), is almost twice higher than the effect of conductive transfer and Ma_T.

Our next article using micro PIV measurements will show that already at short times and for the high temperature T_w, the concentration flow Ma_C will lead to substantially higher velocities in a thin layer of salt solution in comparison with pure water. When approaching the point of the layer rupture (for water) the influence of the thermal convection can be neglected. However, for a very thin layer of aqueous salt solution, the effect of the solutal Marangoni flow may be substantial and must be evaluated.

4. Conclusion

Evaporation and heat mass transfer of the layers of aqueous salt solutions have been studied experimentally. Experimental data of aqueous salt solutions are compared with the water layer.

Aqueous solutions of salts can be divided into two characteristic groups. For water and for the first group of salts (NaCl, CsCl, $BaCl_2$), the evaporation rate j is quasi constant for most part of the evaporation time and heat transfer coefficient increase with time at the end of evaporation. The evaporation rate of salt solutions of $CaCl_2$, LiCl, LiBr and $MgCl_2$ decreases with time. For the second group (NaCl, CsCl, $BaCl_2$), the rate of evaporation falls sharply with increasing salt concentration and with decreasing height of the liquid layer, and the heat transfer coefficient α_l has a pronounced extremum.

The division of salts into two groups can be explained by different values of the equilibrium partial vapor pressure.

In order to determine the group of salts to which the aqueous salt solution should be attributed, it is necessary to consider the following properties of salts: molar mass of salt, the heat of salt dilution and the degree of salt solubility (the beginning point of crystallization). This analysis will help to determine the conditions for modeling the evaporation and heat transfer process. For example, it will become clear whether to consider the diffusion equation or limit to solving the energy and momentum transfer equation. The equation for the evaporation rate for the second group of salts can be considered in the quasi-stationary formulation, i.e. assuming that p_{vs} = const. For the first group of salts, p_{vs} can change by an order of magnitude. In this case, the entire evaporation period can be divided into small intervals, and for each Δt interval one should assume p_{vsi} = const. Thus, the nonstationary problem can be reduced to quasi-stationary even for the first group of salts.

With increasing concentration of salt and when approaching the crystallization point, the role of free convection in the liquid phase decreases sharply. For salt solutions LiBr, $CaCl_2$ and LiCl, a significant excess of convection (α) over conductive heat transfer (λ) is observed for the layer height δ over 1.8–2.0 mm. For pure water, the convective and conductive components are comparable even for δ = 3 mm. This difference for salts is associated with substantial intensification of heat transfer, which is probably associated with the solutal Marangoni flow.

Strong influence of Ma_C on heat and mass transfer in a thin layer and at high temperatures has been detected for the first time and is extremely important for accurate modeling in non-stationary and non-isothermal processes.

Acknowledgments

Experiments related to heat transfer intensification at the interface under the conditions of phase transformations and chemical reactions and were carried out within the framework of the development program in the project of the leading universities of the world 5-100 at the National Research Tomsk Polytechnic University.

Conflict of Interest

The material within this paper, at the author's (authors') responsibility, has not been published elsewhere in this substantial

form nor submitted elsewhere for publication. no copyrighted material nor any material damaging third parties interests has been used in this paper, at the author's (authors') responsibility, without having obtained a written permission.

References

[1] N. Shahidzadeh, J. Desarnaud, Damage in porous media: role of the kinetics of salt (re)crystallization, Eur. Phys. J. Appl. Phys. 60 (2012) 24205.
[2] N. Shahidzadeh-Bonn et al., Salt stains from evaporating droplets, Sci. Rep. 5 (2015) 10335.
[3] V.E. Nakoryakov, N.I. Grigoryeva, Nonisothermal absorption in thermotransformers, Novosibirsk, Nauka, 2010.
[4] S.Y. Misyura, Wall effect on heat transfer crisis, Exp. Therm. Fluid Sci. 70 (2016) 389–396.
[5] S.Y. Misyura, Contact angle and droplet heat transport during evaporation on structured and smooth surfaces of heated wall, Appl. Surf. Sci. 414 (2017) 188–196.
[6] K. Sefiane, S.K. Wilson, S. David, G.J. Dunn, B.R. Duffy, On the effect of the atmosphere on the evaporation of sessile droplets of water, Phys. Fluids 21 (2009) 062101.
[7] F. Carle, S. Semenov, M. Medale, D. Brutin, Contribution of convective transport to evaporation of sessile droplets: empirical model, Int. J. Therm. Sci. 101 (2016) 35–47.
[8] O.A. Kabov, D.V. Zaitsev, D.P. Kirichenko, V.S. Ajaev, Interaction of levitating microdroplets with moist air flow in the contact line region, Nanoscale Microscale Thermophys. Eng. 21 (2017) 60–69.
[9] V.P. Lebedev et al., Effect of flow acceleration and initial turbulence level on velocity fluctuations, Fluid Dyn. 28 (1993) 624–629.
[10] V.S. Ajaev, E.Ya. Gatapova, O.A. Kabov, Stability and break-up of thin liquid films on patterned and structured surfaces, Adv. Colloid Interface Sci. 228 (2016) 92–104.
[11] Y. Wang, Z.-G. Wang, Droplets wetting and evaporating on ethanol-philic micro-structured surfaces, Int. J. Heat Mass Transfer 119 (2018) 704–708.
[12] M. Gao, P. Kong, L.-X. Zhang, J.-N. Liu, An experimental investigation of sessile droplets evaporation on hydrophilic and hydrophobic heating surface with constant heat flux, Int. Commun. Heat Mass Transfer 88 (2017) 262–268.
[13] J. Schmid, I. Zarikos, A. Terzis, N. Roth, B. Weigand, Crystallization of urea from an evaporative aqueous at sub-boiling temperatures and surfaces with different wettability, Exp. Therm Fluid Sci. 91 (2018) 80–88.
[14] V.V. Kuznetsov, A.S. Shamirzaev, Comparative analysis of boiling and condensation heat transfer in upflow for Freon R-21 in minichannels, J. Eng. Thermophys. 24 (2015) 357–361.
[15] V.E. Nakoryakov, S.Y. Misyura, Bubble boiling in droplets of water and lithium bromide water solution, J. Eng. Thermophys. 25 (1) (2016) 24–31.
[16] G. Grossman, Simultaneous heat and mass transfer in film absorption under laminar flow, Int. J. Heat Mass Transfer 26 (1983) 357–371.
[17] T. Meyer, Improvement of the exact analytical solutions for combined heat and mass transfer problems obtained with the Fourier method, Int. J. Refrig. 43 (2014) 133–142.
[18] T. Meyer, F. Ziegler, Analytical solution for combined heat and mass transfer in laminar falling film absorption using first type boundary conditions at the interface, Int. J. Heat Mass Transfer 73 (2014) 141–151.
[19] A.K. Rozentsvaig, Ch.S. Strashinskii, Modeling of heat transfer conditions in cooling lubricant emulsions with low-boiling continuous media in narrow gaps, Int. J. Heat Mass Transf. 102 (2016) 555–560.
[20] H. Lower, Thermodynamische und physikalische Eigenschaften der wassrigen Lithiumbromid-Losung, Dissertation, Karlsruhe, 1960.
[21] K. Ogava, Thermodynamic properties of aqueous solution of lithium bromide, measurement of specific heat at atmospheric pressure, Refrigeration (Japan) 55 (630) (1980) 347–351.
[22] M.R. Conde, Properties of aqueous solution of lithium and calcium chlorides: formulations for use in air conditioning equipment design, Int. J. Therm. Sci. 43 (2004) 367–382.
[23] A.G. Dolotov, V.Yu. Pyatko, Method of calculating thermodynamical and thermophysical properties of aqueous LiBr solution on EDC, in Kholodil'nye mashiny i termotransformatory (Refrigerators and Thermotransformers), LTIKhP, Leningrad, 1985.
[24] J. Ibarra-Bahena, U. Dehesa-Carrasco, R.J. Romero, B. Rivas-Herrera, W. Rivera, Experimental assessment of a hydrophobic membrane-based desorber/condenser with H_2O/LiBr mixture for absorption systems, Exp. Therm Fluid Sci. 88 (2017) 145–159.
[25] N. Hozawa, M. Inoue, J. Sato, T. Imaishi, Marangoni convection during steam absorption into aqueous LiBr solution with surfactant, J. Chem. Eng. Jap. 24 (1991) 209–214.
[26] V.E. Nakoryakov, N.I. Grigoryeva, N.S. Bufetov, R.A., Dekhtyar, Heat and mass transfer intensification at steam absorption by surfactant additives, Int. J. Heat Mass Transfer 51 (2008) 51753–55181.
[27] V.E. Nakoryakov et al., Vapor absorption by immobile solution layer, Int. J. Heat Mass Transfer 47 (2004) 1525–1533.
[28] S.S. Kutateladze, Fundamentals of Heat Transfer Theory, Atomizdat, Moscow, 1979.
[29] D.B. Spalding, The combustion of liquid fuel, 1953. Pittsburgh.
[30] D. Brutin, B. Sobac, F. Rigollet, C. Le-Niliot, Infrared visualization of thermal motion inside a sessile drop deposited onto a heated surface, Exp. Therm. Fluids Sci. 35 (2011) 521–530.
[31] A. Chandramohan, J.A. Weibel, S.V. Garimella, Spatiotemporal infrared measurement of interface temperatures during water evaporation on a nonwetting substrate, Appl. Phys. Lett. 110 (2017) 041605.
[32] H. Groen, K.J. Roberts, An examination of the crystallization of urea from supersaturated aqueous and aqueous-methanol solutions as monitored in-process using ATR FTIR spectroscopy, Cryst. Growth Des. 4 (2004) 930–936.
[33] S.Y. Misyura, Evaporation of a sessile water dropand a drop of aqueous salt solution, Sci. Rep. 7 (2017) 14759.